Research on Chemical Intermediates
https://doi.org/10.1007/s11164-020-04284-8

Cytotoxic effects, microbiological analysis and inhibitory properties on carbonic anhydrase isozyme activities of 2-hydroxy-5-methoxyacetophenone thiosemicarbazone and its Cu(II), Co(II), Zn(II) and Mn(II) complexes

Asuman Ucar, et al. ***[full author details at the end of the article]***

Received: 3 July 2020 / Accepted: 26 September 2020

Abstract

Metal complexes of thiosemicarbazones have been receiving considerable attention in biological applications such as antimicrobial and anticancer therapies. In this work, Co(II), Zn(II) and Mn(II) complexes of 2-hydroxy-5-methoxyacetophenone thiosemicarbazone (HMAT) were synthesized for the first time and characterized by EPR, FT-IR, NMR, UV–Vis spectroscopies, TG/DSC and elemental analysis. X-ray powder diffraction analysis was carried out for Zn(II) complex. HMAT and its Cu(II), Co(II), Zn(II) and Mn(II) complexes were tested as enzyme inhibitory agents. All compounds are effective inhibitor of cytosolic carbonic anhydrase I and II isoforms (hCA I and II) enzymes. IC_{50} values of HMAT and its Cu(II), Co(II), Zn(II) and Mn(II) complexes were determined as 93.35, 324.46, 25.67, 1.06 and 22.36 μM for CA I isozyme and 99.02, 86.64, 57.76, 10.34 and 36.48 μM for CA II isozyme, respectively. The evaluation of potential cytotoxic effects of the compounds was performed against normal epithelial breast mammary gland CRL-4010, estrogen-positive low metastatic MCF-7 and triple negative highly metastatic MDA-MB-231 breast adenocarcinoma cell lines by MTT assay. The results showed that the tested metal complexes have high cytotoxic effects than their ligand molecule. In particular, the Cu(II) complex displayed preciously high cytotoxic properties different from the others. Given these facts, the Cu(II) complex could be debated as potential chemotherapeutic molecule against drug-resistant breast cancer cells. Minimum inhibitory concentrations of the compounds against the test organisms were also detected for the microbiological analysis.

Keywords Thiosemicarbazone · Complexes · Carbonic anhydrase · Antimicrobial and anticancer activity · Spectroscopic and thermal analysis

Electronic supplementary material The online version of this article (https://doi.org/10.1007/s11164-020-04284-8) contains supplementary material, which is available to authorized users.

Published online: 07 October 2020

Introduction

Aromatic thiosemicarbazone analogues were used in medicinal chemistry due to their antiproliferative, antibacterial, antitumor, antifungal and antiviral activities [1–6]. Thiosemicarbazones have antiparasitic and antibacterial effects against many bacterial strains and this can be used in their identification [7]. As the responsible moiety, the conjugated N–N–S system in the thiosemicarbazone scaffolds has been identified for the designated biological properties [8]. Especially with this system, obtaining chelate metal complexes even more increases the biological activity [9]. Copper is a crucial nutrient required for important biological processes [10] such as in redox reactions and required as an allosteric component for many cellular enzymes in all organisms. For example in humans, the essential enzymes that require copper ion as a cofactor for their functions include Cu/Zn superoxide dismutase (SOD), cytochrome c oxidase, ceruloplasmin, lysyl oxidase (LOX) and tyrosinase [11]. The anticancer activity of copper complexes is dependent on generation of highly reactive oxygen species (ROS) by ionic copper due to its redox activation in the cytosol. By this way, free copper could cause damage to cellular biomolecules such as lipids, proteins and nucleic acids. The tumor cells in comparison with normal cells contain raised ROS depending on reduced glutathione mediated antioxidant capacity. Therefore, they have become more sensitive to pro-oxidant ionophoric copper. Accordingly, the copper complexes increased intracellular copper ionophores, producing toxic levels of intracellular ROS in cancer cells, but not in normal cells. The potential for copper molecules to be used as hypoxia markers has been thoroughly evaluated in both preclinical and clinical studies [11, 12]. Recently, it has been determined that cancer cells showed greater copper uptake than normal cells [13]. The copper transporter-1 is known to play a role in the cellular uptake of copper ions and assessed as a new reporter for 64Cu PET imaging in cancer [14].

The carbonic anhydrase enzyme (CA, 4.2.1.1), which contains Zn^{2+} ions in its active site and is commonly found in all organisms, catalyzes the reversible reaction between CO_2 and H_2O that yields H^+ and HCO_3^- [15]. In mammals, there are 17 isoenzymes of CA that are found in cytosol, membrane-bound, mitochondria, extracellular space and saliva, with different catalytic activities and behavior against inhibitors. Of these, CA I and II are cytosolic [16]. CAs have been reported to participate in biological events such as respiration, acid–base and ion homeostasis, tumorigenesis and urea formation [17]. CA I is the most abundant protein in erythrocytes that does not contain hemoglobin and is expressed about 5–6 times more than CA II. Although it has been determined that the deficiency does not cause any abnormality, it can be said that this is due to the presence of CA II [18]. However, Zheng and colleagues reported that CA I expression in breast cancer is increased, induces abnormal cell calcification, apoptosis and migration, and may be a potential oncogene [19]. CA II remains a target for the treatment of diseases such as glaucoma, edema, epilepsy and attitude sickness. In addition, CA II has important roles in thyroid hormone synthesis. CAs have become an interesting enzyme, especially after their inhibitors have been found

to act diuretically [17, 20]. Today the carbonic anhydrases could be inhibited by several compounds such as sulfonamides, sulfonates and sulfamides for cancer and other metabolic disorder therapies. Generally, these chemical inhibitors target the catalytic zinc ion in the enzyme cavity. In particular, indisulam and COUMATE-667 compounds are still under consideration as anticancer agents. Until today, CA inhibitors were commonly used as diuretic and antiglaucoma agents, but turn out that several of them showed significant antitumorigenic effects. However, most of the CA inhibitors show undesirable side effects due to the random or the off target inhibition of CA isoforms [21]. Therefore, specific isozyme selective new compounds with fewer side effects still need to be developed.

Herein we report the synthesis and characterization of Co(II), Zn(II) and Mn(II) complexes of HMAT for the first time. We had synthesized the HMAT and its Cu(II) complex in our previous work and presented their characterizations. In other part of our study, we investigated the antimicrobial, anticancer and carbonic anhydrase inhibition (CA I and II inhibitory) effects of HMAT and of its Cu(II), Co(II), Zn(II) and Mn(II) complexes. According to the results, the biological activities of the compounds were evaluated.

Experimental

Chemistry

All chemicals were of analytical reagent grade. ^{1}H, ^{13}C NMR spectra were recorded with a Bruker AC 400 (400 MHz) NMR spectrometer. For structural analysis of the samples, they were measured in the range of 4000–500 cm^{-1} using attenuated total reflection-Fourier transformed infrared (ATR-FT-IR) spectrometer (PerkinElmer 100). UV–Vis absorption spectrum was obtained on Shimadzu UV-1800 double-beam spectrophotometer. Thermogravimetric analysis (TGA, 25–900 °C) was performed using Setaram thermal gravimetric analyzer at heating rate 10 °C/min and nitrogen flow rate of 20 ml/min. XRD measurements were taken using Bruker axis diffractometer (Bruker D8 ADVANCE) with Cu Kα radiation, operating at 40 kV and 30 mA with a rate of 21 ml/min. EPR spectra of Mn(II) complex in polycrystalline form were investigated using JEOL JesFa300 X-band spectrometer at the 300 and 123 K temperatures, respectively. Carbonic anhydrase enzyme activity was determined by using UV–Vis spectrophotometer—Optizen POP.

Synthesis of HMAT

HMAT was prepared according to our previous article [22]. The general procedure is illustrated in Scheme 1.

Anal. Calcd. For $C_{10}H_{13}N_3O_2S$: C, 50.19; H, 5.48; N, 17.56%. Found: C, 49.91; H, 3.59; N, 17.40%. ^{1}H NMR (400 MHz DMSO-d_6): δ (ppm): 12.62 (*s*, 1H, –OH), 7.1–6.92 (*d*, 2H, H_{Ar}), 3.59–2.38 (*s*, 3H, $–CH_3$). FT-IR (cm^{-1}) υ:, 3388, 3185,

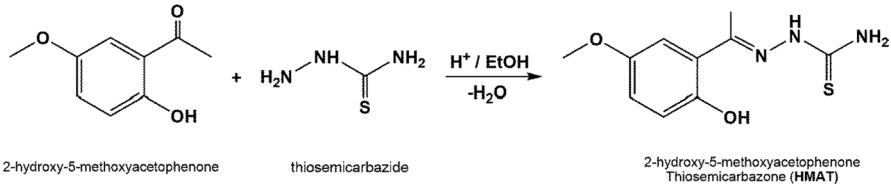

Scheme 1 Synthetic routes for 2-hydroxy-5-methoxyacetophenone thiosemicarbazone (HMAT)

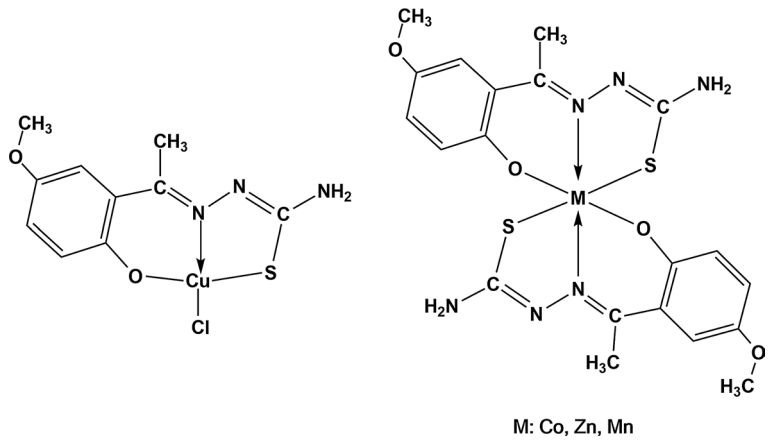

Scheme 2 Proposed structures of complexes

2359, 1646, 826, 539. ^{13}C NMR (400 MHz, $CDCl_3$): δ (ppm): 181.1 (C_1=S), 146.6 (C_2=N), 154.0 (C_3–OH), 114.0–120.1 (C_{Ar}).

Synthesis of metal complexes

Cu(II) complex was prepared according to our previous article [23]. Co(II), Zn(II) and Mn(II) complexes were synthesized for the first time in this study following this general procedure: In an amount of 1:2 metal/ligand molar ratio, $CoCl_2$ $6H_2O$, $ZnCl_2$ and $Mn(NO_3)_2$ $4H_2O$ in the minimum quantity of EtOH were added dropwise to the 3.0 mmol of HMAT in EtOH (60 mL) separately. After refluxing for 2 h, the resulting solids were filtered and washed with anhydrous ether. Physical data of HMAT and its Cu(II), Co(II), Zn(II) and Mn(II) complexes are given in Table 1. The proposed structures of complexes are shown in Scheme 2 considering similar structures in the related publications [24–27].

Table 1 Physical data of HMAT and its Cu(II), Co(II), Zn(II) and Mn(II) complexes

Compound	Color	M.p. (°C)	Yield %
HMAT	Cream	186–188	52
Cu(II)	Dark green	187–189	47
Co(II)	Brown	190–192	43
Zn(II)	Yellow	189–191	48
Mn(II)	Dark red	191–193	41

Cu(II) komplex:

Anal. Calcd. For $C_{10}H_{11}ClCuN_3O_2S$: C, 35.72; H, 3.30; N, 12.50%. Found: C, 35.75; H, 3.50; N, 12.78%. ^{1}H NMR (400 MHz, DMSO-d_6): δ (ppm)): 7.29–6.90 (*d*, 2H, H_{Ar}), 6.59 (*s*, 2H, –NH_2), 3.57–2.58 (*s*, 3H, –CH_3). FT-IR (cm^{-1}) υ: 3487, 3261, 1523, 1262, 824, 526.

Co(II) komplex:

Anal. Calcd. $C_{20}H_{22}N_6O_4S_2Co$: C, 45.03; H, 4.16; N, 15.75%. Found: C, 45.13; H, 4.21; N, 15.78%. %. ^{1}H NMR (400 MHz, DMSO-d_6: δ (ppm): 7.29–6.75 (*d*, 2H, H_{Ar}), 6.90 (*s*, 2H, –NH_2), 3.62–2.52 (*s*, 3H, –CH_3). FT-IR (cm^{-1}) υ: 3522, 3099, 1537, 1217, 1031, 783, 590.

Zn(II) komplex:

Anal. Calcd. $C_{20}H_{22}N_6O_4S_2Zn$: C, 44.49; H, 4.11; N, 15.56%. Found: C, 45.03; H, 4.19; N, 15.68%. ^{1}H NMR (400 MHz, DMSO-d_6): δ (ppm): 7.24 (*s*, 2H, –NH_2), 6.93–6.84 (*d*, 2H, H_{Ar}), 3.78–2.35 (*s*, 3H, –CH_3). FT-IR (cm^{-1}) υ: 3486, 3192, 1540, 1215, 1030, 783, 585.

Mn(II) komplex:

Anal. Calcd. $C_{20}H_{22}N_6O_4S_2Mn$: C, 45.37; H, 4.19; N, 15.87%. Found: C, 45.53; H, 4.29; N, 15.98%. ^{1}H NMR (400 MHz, DMSO-d_6): δ (ppm): 7.63–7.29(*d*, 2H, H_{ar}), 7.15 (*s*, 2H, –NH_2), 3.73–2.34 (*s*, 3H, –CH_3). FT-IR (cm^{-1}) υ: 3351, 3190, 1629, 1200, 1028, 783, 583.

Purification of CA I, II and esterase activity assay

CA I and II enzymes were purified from human erythrocytes using the method described earlier by Kuzu and co-workers [28]. Erythrocytes were obtained from Agri State Hospital blood bank. Enzyme activity was measured spectrophotometrically at 348 nm using 4-nitrophenyl acetate as substrate [29].

Microbiological analysis

The following species of bacteria were used in the study for the microbiological analysis: *Staphylococcus aureus* ATCC 25,923, *S. Aureus* ATCC 43,300 (Resistant to methicillin), *Enterococcus faecalis* ATCC 29,212, *Escherichia coli* ATCC 25,922, *Salmonella enteriditis* ATCC 13,076, *Pseudomonas aeuroginosa* ATCC 2783, *P. Aeuroginosa* ATCC 2783 and *Candida albicans* ATCC90028 (yeast). Minimum inhibitory concentrations (MICs) of HMAT and its Cu(II), Co(II), Zn(II) and Mn(II) complexes against the test organisms were detected according to the recommendations of the Clinical and Laboratory Standards Institute [30].

Cell viability assay

To evaluate the cytotoxic effects of HMAT and its Cu(II), Co(II), Zn(II) and Mn(II) complexes on CRL-4010, MCF-7 and MDA-MB-231 cell lines, the cells were cultured in complete DMEM (Dulbecco's modified Eagle medium) (Sigma) and seeded into 96-well plates (Costar, Corning Inc) at a density of 1×10^4 cells per well. After overnight culturing, the cells were treated with the ligand and its complexes at a final concentration of 0.78, 1.56, 3.12, 6.25, 12.5, 25 and 50 µM in 100 µl medium for 72 h. Control cells were treated with DMSO simultaneously. All doses of tested compounds and control wells were performed in triplicate. At the end of treatment, 10 µL thiazolyl blue tetrazolium bromide (MTT) was added to each well and incubated for 4 h. Then supernatants were discarded and DMSO was added to dissolve formazan. The optical density values of each well were determined by spectrophotometer (Multiscan GO, Thermo Fisher Inc.) at 570 and 690 nm. The % cell viability of the samples was calculated by using the following formula: % cytotoxicity = (1—the mean OD of experimental wells)/(the mean OD of control wells) × 100%. The IC_{50} values of the ligand and its metal complexes for CRL-4010, MCF-7 and MDA-MB-231 cells were estimated separately from the data of generated dose–response curve.

Statistical analysis

The IC_{50} values of each compound were calculated by logarithmic mean of the percentage of inhibition concentrations, and 95% confidence interval (CI) values and mean ± standard errors (SEM) were determined by using the GraphPad Prism8 software.

Results and discussion

Characterizations of compounds

^{1}H NMR, FT-IR and TGA analyses of HMAT and its Cu(II) complex have been reported in our previous studies [22, 23]. Detailed characterization of the first synthesized Co(II), Zn(II) and Mn(II) complexes is given below.

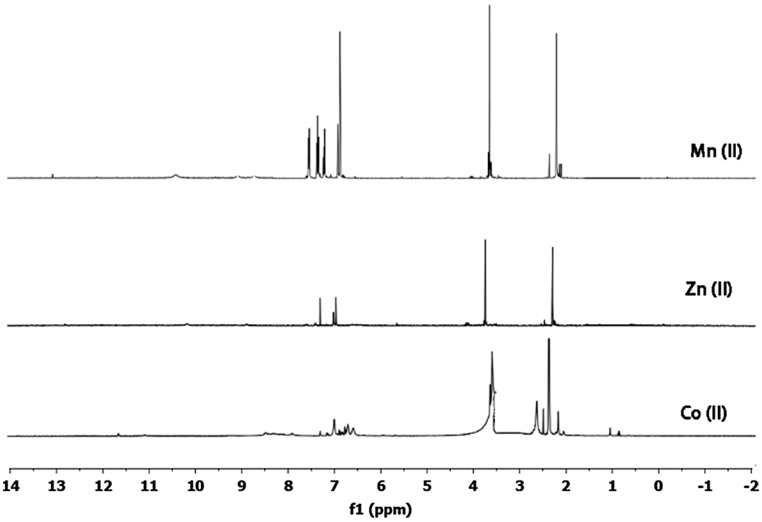

Fig. 1 ^{1}H NMR spectra of Co(II), Zn(II) and Mn(II) complexes

In the ^{1}H NMR spectra of Co(II), Zn(II) and Mn(II) complexes (Fig. 1), -OH (12.62 ppm) and –NH signal (11.12 ppm) of HMAT (Fig. S1) [31, 32] were disappeared due to the coordination of the deprotonated phenolate component after the complexation. The proton signal of the $–NH_2$ of Co(II), Zn(II) and Mn(II) complexes was appeared as a singlet at 6.90, 7.24, 7.15 ppm, respectively [33, 34]. The protons in the aromatic ring have signals in the range of 6.75–7.63 ppm for the complexes. A singlet was appeared at 3.62, 3.78, 3.73 ppm for the proton present in the methoxy group [35], and a singlet appeared around 2.52, 2.35, 2.34 ppm was attributed to CH_3 proton of azomethine group [36] for Co(II), Zn(II) and Mn(II) complexes, respectively.

^{13}C NMR spectrum of HMAT is shown in Fig. S2. The signals for the carbon atom of C = S group and C–OH were appeared at 181.1 and 154.0 ppm, respectively. The signals at the range of 114.0–120.1 ppm can be attributed to aromatic carbons (C_{AR}). The obtained results are compatible with the studies [37, 38].

The FT-IR spectra of the complexes and HMAT are shown in Fig. 2a and Fig. S3, respectively. υ(O–H) and υ(N–H) vibrations, which are the characteristic peaks of thiosemicarbazone and disappeared in the complexes, have been found at 3388 cm^{-1} and 3185 cm^{-1} for HMAT (Fig. S3), respectively [36]. $\upsilon(–NH_2)$ stretching frequencies have been found between 3522–3351 cm^{-1} in all complexes [36]. The band observed at 826 cm^{-1} in HMAT which attributed to ν(C = S) was not seen in the spectrum of the complexes. A new group appeared at higher energy (783 cm^{-1}) indicating coordination of sulfur atom to metal [39]. Other characteristic peak υ(C = N) was observed at 1537 cm^{-1} for Co(II), 1540 for Zn(II) and 1629 for Mn(II) [27]. After complexation, metal-O vibrations in the complexes around 590 cm^{-1} evidence the coordination through oxygen [40].

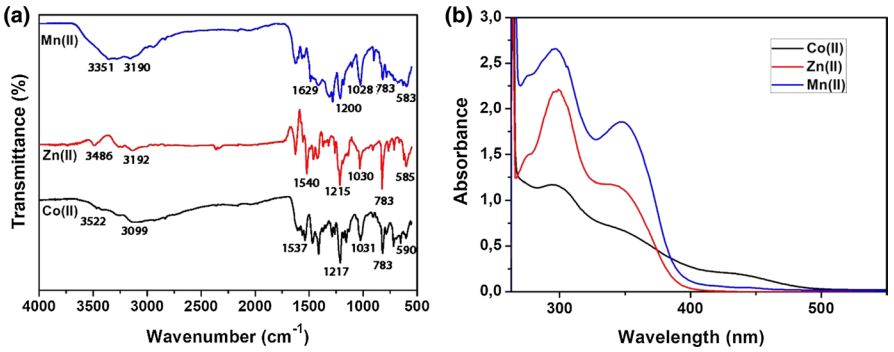

Fig. 2 FT-IR **a** and UV–Vis **b** spectra of Co(II), Zn(II) and Mn(II) complexes

In the UV–Vis spectra of HMAT (Fig. S4), the band at 305 nm was assigned to π—π* transitions of azomethine, while the absorption at 355 nm corresponds to a n—π* transition of thioamide [22]. The absorption bands of the complexes (Fig. 2b) appear at 295–298 nm owing to π—π*, and the other one at 343–347 nm corresponds to n—π* transitions. By comparing the frequency of HMAT and the corresponding complexes, the electronic transitions of π—π* are shifted to a lower value due to the formation of the complexes and coordination of the ligand to the metal.

TG/DSC curve of new synthesized Co(II), Zn(II) and Mn(II) complexes is represented in Fig. 3. The Co(II) complex is stable up to 200 °C, indicating the absence of water. The first weight loss at 310 °C (Cald; 10.22%, Obs; 10.17%) can be attributed disintegrated units of ligand molecules [41]. The other weight loss due to the residue of the product can be seen in the range of 375 °C and 450 °C (Cald; 3.77%, Obs; 3.86%). The Zn(II) complex is stable up to 180 °C, indicating the absence of water. The first weight loss at 225 °C (Cald; 10.11%, Obs; 10.14%) can be attributed disintegrated units of ligand molecules. The other weight loss due to the residue of the product can be seen in the range of 275 °C and 375 °C (Cald; 50.77%, Obs; 50.86). The first stage of the TG degradation of the Mn(II) complex was from 69–118 °C, which corresponded to the lost of lattice water (Cald; 6.37%, Obs; 6.87). The other weight loss due to the residue of the product decomposition can be seen in the range of 200 °C and 290 °C (Cald; 19.74%, Obs; 19.96%). The decomposition of the complexes to CoO, ZnO and

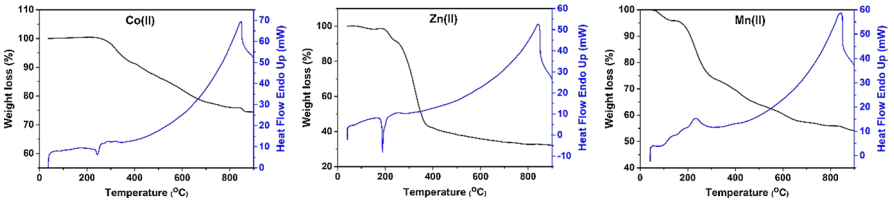

Fig. 3 TG/DSC curve of Co(II), Zn(II) and Mn(II) complexes

MnO starts within the temperature ranging from 500 °C to 800 °C. As can be seen in the DSC curve of Co(II), Zn(II) and Mn(II) complexes, a single peak observed at 243.06 °C, 188.38 °C, 234.46 °C, respectively, indicates that compounds were obtained in pure form.

EPR analysis of complexes

EPR, a nondestructive spectroscopic method, can be directly used to detect and characterize the paramagnetic centers having unpaired electron(s) such as transition metals [42]. Detailed EPR spectrum examination of Cu(II) complex of HMAT was done in our previous study [23]. The EPR spectrum of Zn(II) complex of HMAT could not be studied since Zn(II) is not paramagnetic. The EPR spectrum shown in Fig. 4 recorded at 300 K has broadened isotropic EPR signal with the value $\Delta H_{pp} = 64.13$ mT. This can be interpreted as enhanced spin lattice relaxation due to dipolar interaction and random orientation of Mn (II) ions [43]. In order to eliminate unwanted effects and obtain the spectra with the highest resolution, powdered complex was diluted in DMF and EPR spectra were recorded at 123 K. Due to the hyperfine interaction between the unpaired electron and metal nuclear spins (^{55}Mn, $I = 5/2$) of the complex, a hyperfine sextet was observed at the spectrum given in Fig. 5. By considering the resonance condition $g_{iso} = h\upsilon/g\beta H_r$, the g_{iso} value was measured as 2.0036 which is very close to free electron spin value suggestive of the absence of spin orbit coupling in the ground state. The average value of hyperfine splitting for allowed transitions corresponding to $\Delta m_I = 0$ was measured as 9.5 mT. This value is consistent with octahedral coordination because in tetrahedral sites A_{iso} is 20–25% lower than octahedral sites. In addition to allowed transitions, between each of the two main hyperfine lines a pair of low-intensity forbidden lines with an average spacing of 2.3 mT is observed corresponding to $\Delta m_I = \pm 1$ transitions [44]. This forbidden line is observed because of the mixture of the nuclear hyperfine levels by the zero-field splitting factor of the Hamiltonian [45]. The measured values of main line splitting from low to high field (8.8, 9.3, 9.5, 9.8 10.1 mT) and the doublet

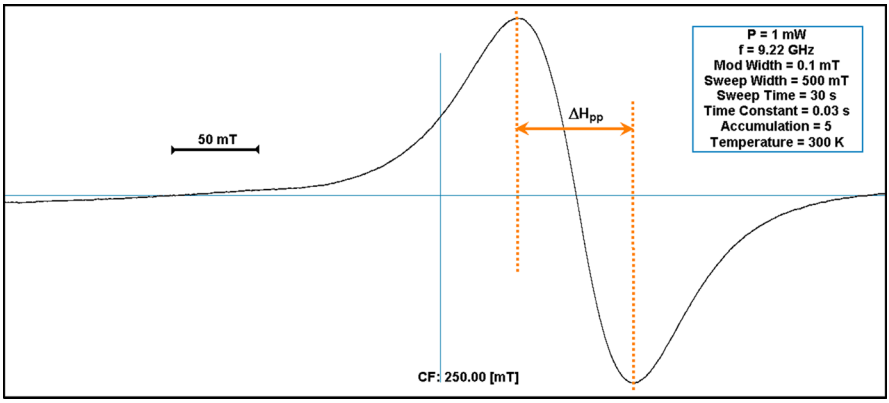

Fig. 4 Powder EPR spectrum of Mn(II) complex at 30 0 K temperature ($\Delta H_{pp} = 64.13$ mT)

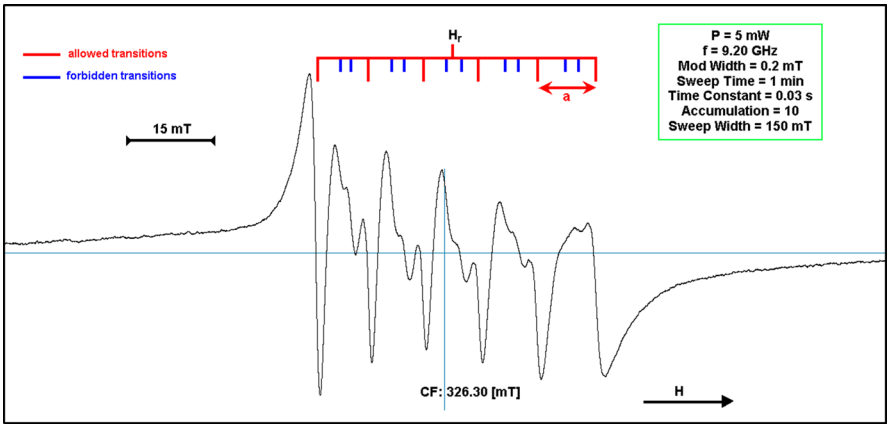

Fig. 5 EPR spectrum of Mn(II) complex at 123 K temperature in frozen DMF solution

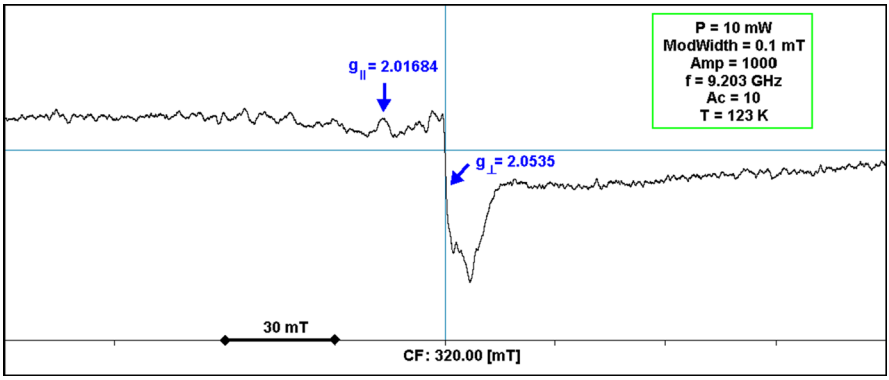

Fig. 6 EPR spectrum of Co(II) complex in frozen DMF solution at 123 K temperature

splitting from low to high field (1.9, 2.2, 2.5, 2.4, 2.5 mT) are in good agreement with the values given in the literature [46]. The magnetic moment was determined as 5.93 B.M using the $\mu = g_{iso}[S(S+1)]^{1/2}$ equation which supports the d^5 high-spin Mn(II) complex [47].

EPR spectra of Co(II) complex were recorded at 123 K in frozen DMF solution using the JEOL JesFa300 X-band spectrometer (Fig. 6). An axially symmetric spectral pattern was obtained at this temperature which supports the low-spin complex with $S = 1/2$ since for the high-spin complexes with $S = 3/2$ very low temperatures are necessary due to the short spin-lattice relaxation time [48]. The parallel and perpendicular components of the spectroscopic splitting value were measured as $g_{||} = 2.1684$ and $g_{\perp} = 2.0535$, and the order $g_{||} > g_{\perp} > g_e$ indicates the presence of unpaired electron in $d_{x^2-y^2}$ orbital [49].

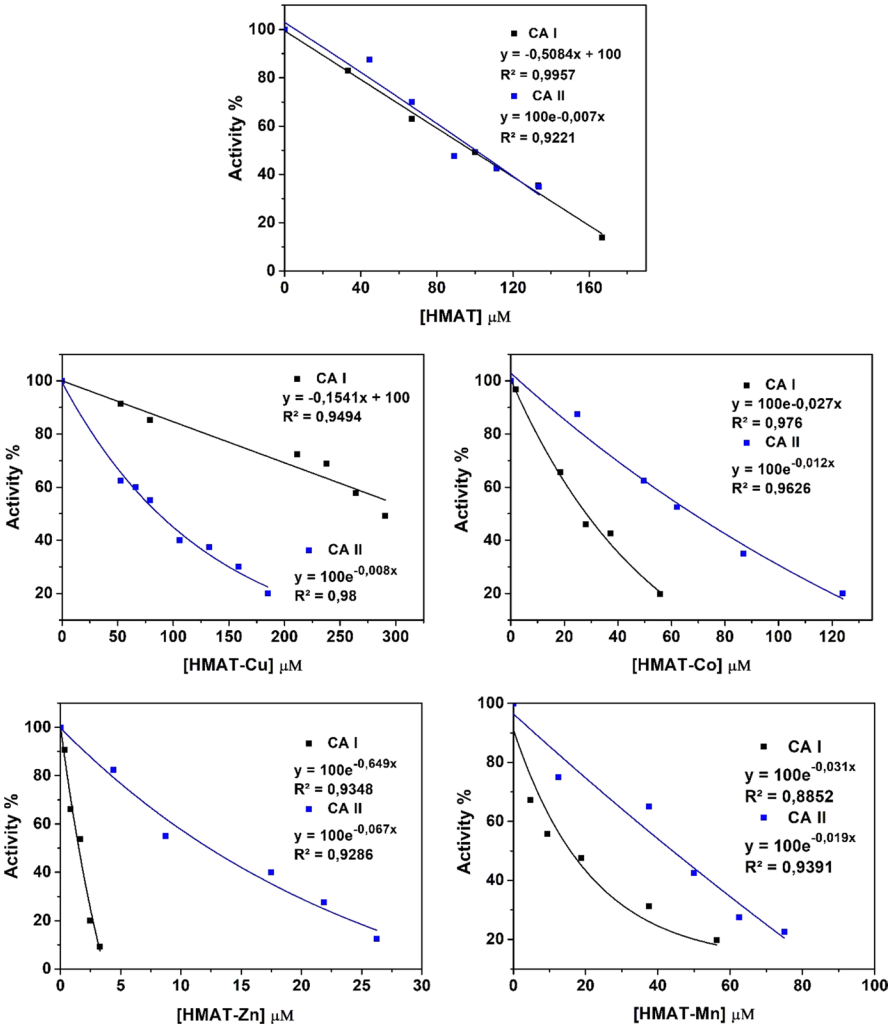

Fig. 7 % Activity–[I] plots for HMAT and its Cu(II), Co(II), Zn(II) and Mn(II) complexes having inhibition effect

Table 2 IC_{50} values of HMAT and its Cu(II), Co(II), Zn(II) and Mn(II) complexes on CA I and CA II isoenzymes

Compound	IC_{50} CA I (μM)	IC_{50} CA II (μM)
HMAT	98.35	99.02
Cu(II)	324.46	86.64
Co(II)	25.67	57.76
Zn(II)	1.06	10.34
Mn(II)	22.36	36.48

Carbonic anhydrase inhibition

In order to determine the effects of HMAT and its Cu(II), Co(II), Zn(II) and Mn(II) complexes on enzymatic activity, activity measurements were taken at five different concentrations. % Activity–[compound] graphs were drawn using the results obtained by taking control measurement as 100% (Fig. 7). The concentration of substance causing 50% inhibition was calculated from the graph equation. Accordingly, the Zn(II) complex showed the strongest inhibitory effect for both CA I and CA II. The results are summarized in Table 2.

Cytosolic CA II is the most widely spread isoenzyme and is found in almost all tissues. The main role of CA II is to promote H^+ production and acid–base homeostasis, pH balance and metabolic acidosis [50]. It has been reported that CA I plays an important role in the formation of retinal and cerebral edema, and its inhibition may be advantageous in the elimination of these conditions [51]. CA I has been shown to be an indicator for differentiating autoimmune hemolytic anemia from other types of anemia [52]. In addition, it has been reported that CA I and II are associated with gastrointestinal tumors, and CA II may be a novel biomarker for gastrointestinal stromal tumors [53]. It has been stated that CA enzymes are important therapeutic targets and that both their inhibitors and activators are already used as drugs. Approximately 25 drugs have been developed that are used clinically and targeting CAs, utilized as diuretics, antiglaucoma, anticonvulsant and anticancer [50]. Besides, CA inhibitors have been shown to be antifungal and bacterial agents [54]. Previous studies have identified natural and synthetic substances that have an in vivo or in vitro inhibitory effect on CA, and have also reported that some metal ions inhibit the enzyme [51, 55–57]. Therefore, synthesis of new and potent CA inhibitors is important.

Microbiological analysis

HMAT and its Cu(II), Co(II), Zn(II) and Mn(II) complexes have bacteriostatic activity on tested organism at different degrees (Table 3). Although antibacterial activity

Table 3 MIC values of HMAT and its Cu(II), Co(II), Zn(II) and Mn(II) complexes

Test organisms	MIC (mg/ml)					
		HMAT	Cu(II)	Co(II)	Zn(II)	Mn(II)
C. Albicans ATCC90028	Yeast	0.31	0.31	1.25	0.31	0.31
S. Enteriditis ATCC 13,076	Gram-negative	1.25	1.25	1.25	1.25	1.25
P. Aeuroginosa ATCC 2783		1.25	0.625	1.25	1.25	1.25
Klebsiella pneumoniae ATCC 70,060		1.25	1.25	1.25	1.25	1.25
E. Coli ATCC 25,922		2.5	2.5	1.25	2.5	1.25
E. Faecalis ATCC 29,212	Gram-positive	1.25	0.31	1.25	1.25	0.31
S. Aureus ATCC 25,923		2.5	2.5	1.25	2.5	2.5
S. Aureus ATCC 43,300 (Resistant to methicillin)		2.5	2.5	2.5	2.5	2.5

of HMAT on *C. Albicans* and gram-positive bacteria was not observed, Zn(II) and Cu(II) complexes have antibacterial effect on these microorganisms. The inhibitory effects of the Mn(II) and Co(II) complexes on *C. Albicans* are particularly noteworthy.

In previous studies [58–61], the in vitro antibacterial activity of the different thiosemicarbazone complexes was shown against gram-positive and gram-negative bacteria and also fungi in different concentrations. Noruzi et al. (2020) [62] were detected a considerable antibacterial activity against gram-positive and gram-negative bacteria in particular $MIC = 31.25$ µg/mL concentration of thiosemicarbazone complexes. Similar to our study, they reported the fungal strains were resistant against complexes except for cobalt complex.

Evaluation of anticancer activity on breast cancer cell lines

The cytotoxic properties of HMAT and its Cu(II), Co(II), Zn(II) and Mn(II) complexes against normal breast epithelium CRL-4010, low metastatic MCF-7 and highly metastatic MDA-MB-231 cells were assessed by MTT assay (Fig. 8). By all accounts, the IC_{50} values and their 95% confidence intervals (CI) of each compound were calculated by GraphPad Prism8 software (Table 4). According to the results, metal complexes have higher toxic properties than their ligand. Also, the tested compounds were found to have weaker cytotoxic effects on normal cells than on MCF-7 and MDA-MB-231 breast cancer cells. Among these metal complexes, the Cu(II) complex was found as the highest cytotoxic compound. In detail, the IC_{50} value of HMAT on normal cells was 234.5 µM, while the IC_{50} value on cancer cells was 210.2 µM on MCF-7 and 110.7 µM on MDA-MB-231 cells. The IC_{50} values of Co(II), Zn(II) and Mn(II) complexes were ranged at 115.3–228 µM on normal cells, 46.77–103.4 µM on MCF-7 cells and 36.92–71.82 µM on MDA-MB-231 cells. Remarkably, the IC_{50} values of Co(II) complex were ranging from 0.8 to 2.6 µM at the tested cell lines. By last result, the Cu(II) complex was determined to have 30–120 times higher cytotoxic properties than the other compounds. For benchmarking of these effects, the chemosensitivity (IC_{50} values) of the first and widely used metal (platinum)-containing drug, cisplatin (cis-diammineplatinum(II) dichloride), is known to be 97.86 µM for MCF-7 and 36.20 µM for MDA-MB-231 cell line. In this direction, it could be generalize that the tested Cu(II) complex was highly cytotoxic 113-fold to MCF-7 and 30-fold to MDA-MB-231 cells than cisplatin. In addition, the

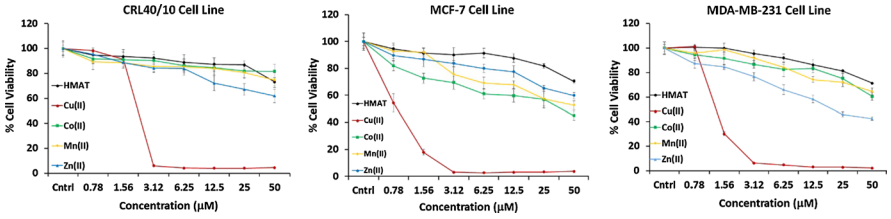

Fig. 8 Cytotoxic properties of HMAT and its Cu(II), Co(II), Zn(II) and Mn(II) complexes against normal breast epithelium CRL-4010, low metastatic MCF-7 and highly metastatic MDA-MB-231 cells

Table 4 IC_{50} (μM) and 95% confidence interval (CI) values of HMAT and its Cu(II), Co(II), Zn(II) and Mn(II) complexes against normal breast epithelium CRL-4010, low metastatic MCF-7 and highly metastatic MDA-MB-231 cells

IC_{50} values (μM)					
Cell lines	HMAT	Cu(II)	Co(II)	Zn(II)	Mn(II)
CRL-4010	234.5	2.615	228	115.3	174.7
	(95% Cl:159.3–397-4)	(95% Cl:1.2295–4.96)	(95% Cl:156.6–377.6)	(95% Cl:7.76–187.8)	(95% Cl:123.2–272)
MCF-7	210.2	0.865	46.77	103.4	64.8
	(95% Cl:17.73–334.4)	(95% Cl:0.0523–1.272)	(95% Cl:34.99–63.62)	(95% Cl:74.50–151.9)	(95% Cl:50–86.17)
MDA-MB-231	110.7	1.203	66.34	36.92	71.82
	(95% Cl:90.97–137.7)	(95% Cl:0.07337–1.898)	(95% Cl:49.75–91.42)	(95% Cl:27.76–49.44)	(95% Cl:51.43–104)

another prominent complex that we regard as significant was Zn(II) complex, due to exert similar cytotoxic properties to cisplatin. In brief, it could be said that the our synthesized metal complexes have at least as much cytotoxic effects as cisplatin.

Currently, the screening for effective chemotherapeutic agents for the treatment of drug-resistant tumor cells is ongoing. In addition, the search for novel adjuvant molecules that will increase the effect of existing drugs continues rapidly. For this purpose, in this study we investigated the possible anticancer effects of HMAT and its new metal complexes. In light with our findings, the metal complexes were more cytotoxic than their ligand and had a higher cytotoxic effects against MCF-7 and MDA-MB-231 breast cancer cell lines compared to normal breast epithelial cells. With this aspect, our findings were clearly remarkable. A notable consequence was that the Cu(II) complex had an extremely high anticancer activity than the other metal complexes. Copper is an essential nutrient which is important in several biochemical processes and by this regard required by all living organisms. Copper is a transition metal that could transform from the oxidized form (Cu^{2+}) to the reduced form (Cu^{+}) of copper. Due to this redox activity in cytosol, copper is an essential cofactor for many enzymatic processes and pathways. Also it could be considered potentially toxic to the cells when it is in excess amount. This high redox activity of copper could elevate reactive oxygen species (ROS) in the cytosol. When there is an imbalance between the number of ROS formed and the neutralization of these by antioxidant defenses, there is evidence that the toxicity of copper causes oxidative stress. By this way, the intracellular oxidative stress could cause cellular damage through the effects of ROS attack on macromolecules such as sugars, DNA, proteins and lipids [63]. Due to these biological properties of the copper ion, it could be extrapolated that why we find out higher cytotoxic properties in the copper complex. Moreover, remarkably the Zn(II) complex showed approximately 2.8-fold higher cytotoxic effects on MDA-MB-231 cells compared to MCF-7 cells and approximately 3.1-fold higher than normal breast epithelium cells.

Conclusion

The synthesis of thiosemicarbazone ligand containing 2-hydroxy-5-methoxyacetophenone (HMAT) and its Cu(II) complex has been included in our previous studies, while Co(II), Zn(II) and Mn(II) complexes were synthesized for the first time. In this study, inhibition effects of synthesized thiosemicarbazone and its metal complexes on CA I and II enzymes which are therapeutic target in the treatment of some diseases were revealed. According to our results, we found that the Zn(II) complex had higher inhibitory effect against CA I and II enzymes among other metal complexes. In this regard, it is thought that these synthesized substances may be promising for the discovery of new and more potent CA inhibitors.

Copper complexes are promising new more effective drugs for the treatment of patients with aggressive cancer and to overcome cisplatin resistance. Metallotherapeutic drugs, such as cisplatin, cause undesirable side effects and resistance to cisplatin hampered clinical use of these metallotherapeutic agents. Therefore, the studies are still continuing to discover new metallotherapeutic drugs such as copper

complexes with strong anticancer activity for drug-resistant cancer treatment [64]. Considering cytotoxic properties of the compounds, in particular, the Cu(II) complex displayed preciously strong cytotoxic. Given these facts, the Cu(II) and Zn(II) complexes could be debated as potential chemotherapeutic molecule against drug-resistant breast cancer cells. Microbiological findings indicate that synthesized products may become useful for the development of new antibacterial agents.

Acknowledgements This study was supported by the Necmettin Erbakan University Scientific Research Foundation (BAP-161715001)

Compliance with ethical standards

Conflict of interest The authors declare that they have no conflict of interest.

References

1. J. Deng, T. Li, G. Su, Q.-P. Qin, Y. Liu, Y. Gou, J Mol Struct **1167**, 33 (2018)
2. D.S. Kalinowski, P. Quach, D.R. Richardson, Med Chem **1**, 1143 (2009)
3. N.S.H.N. Moorthy, N.M.F.S.A. Cerqueira, M.J. Ramos, P.A. Fernandes, Recent Pat Anticancer Drug Discov **8**, 168 (2013)
4. E. Bozgeyik, D. Tasdemir-Kahraman, K. Arman, I. Bozgeyik, A. Karakucuk-Iyidogan, E.A. Cakmak, Gene Rep **18**, 100578 (2020)
5. H. Muğlu, Res Chem Intermed **46**, 2083 (2020)
6. Z. Bakherad, M. Safavi, A. Fassihi, H. Sadeghi-Aliabadi, M. Bakherad, H. Rastegar, J.B. Ghasemi, S. Sepehri, L. Saghaie, M. Mahdavi, Res Chem Intermed **45**, 2827 (2019)
7. W.M. Elhusseiny, Polycycl Aromat Compd **0**, 1 (2020)
8. M. Bingul, E. Şenkuytu, M.F. Saglam, M. Boga, H. Kandemir, I.F. Sengul, Res Chem Intermed **45**, 4487 (2019)
9. R.V. Singh, P. Chaudhary, S. Chauhan, M. Swami, Spectrochim Acta Part A Mol Biomol Spectrosc **72**, 260 (2009)
10. L.N. Sharada, S.N.T. Sunitha, M. Sabha, T.L. Viveka, Y. Aparna, M. Prasad, Res Chem Intermed **46**, 3341 (2020)
11. D. Denoyer, S.A.S. Clatworthy, M.A. Cater, Met Ions Life Sci **18**, 469 (2018)
12. H. Karlsson, M. Fryknäs, S. Strese, J. Gullbo, G. Westman, U. Bremberg, T. Sjöblom, T. Pandzic, R. Larsson, P. Nygren, Oncotarget **8**, 30217 (2017)
13. J.B. Foo, M.L. Low, J.H. Lim, Y.Z. Lor, R. Zainol Abidin, V. Eh Dam, N. Abdul Rahman, C.Y. Beh, L.C. Chan, C.W. How, Y.S. Tor, L. Saiful Yazan, Biometals **31**, 505 (2018)
14. K. Il Kim, S.J. Jang, J.H. Park, Y.J. Lee, T.S. Lee, K.S. Woo, H. Park, J.G. Choe, G. Il An, J.H. Kang, J Nucl Med **55**, 1692 (2014)
15. M. Kuzu, R. Demirdağ, A. Özkaya, V. Çomaklı, Z. Şahin, U. Dardağan, K. Uzun, M. Koca, J Biol Chem **44**, 409 (2016)
16. X. Liu, D. Lu, R. Bowser, J. Liu, Int J Mol Sci **17**, 1820 (2016)
17. A. Alver, A. Mentes, S.C. Karahan, C. Erem, E.E. Keha, M.K. Arikan, M.S. Eminag, O. Deger, Exp Clin Endocrinol Diabetes **115**, 287 (2007)
18. W.S. Sly, P.Y. Hu, Annu Rev Biochem **64**, 375 (1995)
19. Y. Zheng, B. Xu, Y. Zhao, H. Gu, C. Li, Y. Wang, X. Chang, BMC Cancer **1**, 1 (2015)
20. M. Jakubowski, E. Szahidewicz-krupska, A. Doroszko, BioMed Res Int **2018** (2018)
21. S.M.I. Morsy, A.M. Badawi, A. Cecchi, C.T. Supuran, A. Cecchi, J J Enzyme Inhib Med Chem **24**, 499 (2009)
22. E.G. Akgemci, A.O. Saf, H.U. Tasdemir, E. Türkkan, H. Bingol, S.O. Turan, M. Akkiprik, Spectrochim Acta Part A Mol Biomol Spectrosc **136**, 719 (2015)
23. E. Türkkan, U. Sayin, N. Erbilen, S. Pehlivanoglu, G. Erdogan, H.U. Tasdemir, A.O. Saf, L. Guler, E.G. Akgemci, J Organomet Chem **831**, 23 (2017)

24. A.B.M. Ibrahim, M.K. Farh, S.A. ElGyar, M.A. ELGahami, D.M. Fouad, F. Silva, I.C. Santos, A. Paulo, Inorg Chem Commun **96**, 194 (2018)
25. C.C. Gatto, M.A.S. Chagas, I.J. Lima, F. Mello Andrade, H.D. Silva, G.R. Abrantes, E.P.S. Lacerda, Transit Met Chem **44**, 329 (2019)
26. M. Selvaganapathy, N. Raman, J Chem Biol Ther **01**, 108 (2016)
27. M.S. Refat, H.K. Ibrahim, S.Z.A. Sowellim, M.H. Soliman, E.M. Saeed, J Inorg Organomet Polym Mater **19**, 521 (2009)
28. M. Kuzu, V. Çomaklı, E. Akkemik, M. Çiftci, Ö.İ. Küfrevioğlu, Fish Physiol Biochem **44**, 1119 (2018)
29. J.A. Verpoorte, S. Mehta, J.T. Edsall, J Biol Chem **242**, 4221 (1967)
30. J.B. Patel, R.F. Cockerill, A.P. Bradford, M.G. Eliopoulos, A.J. Hindler, G.S. Jenkins, S.J. Lewis, B. Limbago, A.L. Miller, P.D. Nicolau, M. Pwell, M.J. Swenson, M.M. Traczewski, J.D. Turnidge, CLSI Clin Lab Stand Inst **35**, 1 (2015)
31. Ş. Güveli, I. Kılıç-Cıkla, B. Ülküseven, M. Yavuz, T. Bal-Demirci, J Mol Struct **1173**, 366 (2018)
32. R.A. Bedier, T.A. Yousef, G.M. Abu El-Reash, O.A. El-Gammal, J Mol Struct **1139**, 436 (2017)
33. D. Sharma, J.P. Jasinski, V.A. Smolinski, M. Kaur, K. Paul, R. Sharma, Inorganica Chim Acta **499**, 119187 (2020)
34. R. Konakanchi, J. Haribabu, J. Prashanth, V.B. Nishtala, R. Mallela, S. Manchala, D. Gandamalla, R. Karvembu, B.V. Reddy, N.R. Yellu, L.R. Kotha, Appl Organomet Chem **32**, 1 (2018)
35. M.A. Arafath, F. Adam, M.R. Razali, L.E. Ahmed Hassan, M.B.K. Ahamed, A.M.S.A. Majid, J Mol Struct **1130**, 791 (2017)
36. I. Kılıç-Cıkla, Ş. Güveli, M. Yavuz, T. Bal-Demirci, B. Ülküseven, Polyhedron **105**, 104 (2016)
37. L. V Kumar, S. Sunitha, G. Rathika Nath, Mater. Today Proc. (2020 in press) https://doi.org/10.1016/j.matpr.2020.05.376
38. A. Dehno Khalaji, E. Shahsavani, N. Feizi, M. Kučeráková, M. Dušek, R. Mazandarani, A. Amiri, Comptes Rendus Chim **20**, 125 (2017)
39. O. Abdullahi, W. Handy, M. Shazwan, S. Jamil, M. Shamsuddin, Mal J Fund Appl Sci **16**, 351 (2020)
40. M.A. Affan, M.A. Salam, F.B. Ahmad, F. White, H.M. Ali, Inorganica Chim Acta **387**, 219 (2012)
41. S. Paswan, M.K. Bharty, P. Bharati, P.K. Sonkar, V. Ganesan, R.J. Butcher, New J Chem **41**, 15466 (2017)
42. A. Abragam, B. Bleaney, *Electron paramagnetic resonance of transition ions* (Clarendon Press, UK, 1970)
43. V.L. Siji, M.R.S. Kumar, S. Suma, M.R.P. Kurup, Spectrochim Acta Part A Mol Biomol Spectrosc **76**, 22 (2010)
44. V. Philip, V. Suni, M.R. Prathapachandra, Spectrochim Acta Part A Mol Biomol Spectrosc **64**, 171 (2006)
45. B. Bleaney, R.S. Rubins, Proc Phys Soc **77**, 103 (1961)
46. L. Burlamacchi, E. Tiezzi, Chem Phys Lett **4**, 173 (1969)
47. C.G. Oliveira, P. Ivo, S. Maia, P.C. Souza, F.R. Pavan, C.Q.F. Leite, R.B. Viana, A.A. Batista, O.R. Nascimento, V.M. De, J Inorg Biochem **132**, 21 (2014)
48. A.C. Rizzi, N.I. Neuman, P.J. González, C.D. Brondino, Eur J Inorg Chem **2016**, 192 (2016)
49. A. Sasmal, E. Garribba, V. Ugone, C. Rizzoli, S. Mitra, Polyhedron **121**, 107 (2017)
50. MdI Hassan, B. Shajee, A. Waheed, F. Ahmad, S. William Sly, Bioorg Med Chem **21**, 1570 (2012)
51. L. Safarova, A. Sujayev, I. Gulc, M. Abbasova, P. Taslimi, S.H. Alwasel, C.T. Supuran, V. Farzaliyev, J Enzyme Inhib Med Chem **32**, 1174 (2017)
52. W. Kuo, S. Yang, Y. Hsieh, C. Tsai, H. Wen-Li, C. Shu-Chen, Clin Chim Acta **351**, 79 (2005)
53. A. Mentese, E. Fidan, A. Alver, S. Demir, S.O. Yaman, A. Sumer, S. Fidan, H. Kavgaci, I. Turan, Clin immunol **42**, 73 (2017)
54. H.M. Becker, M. Klier, J.W. Deitmer, *Carbonic anhydrase: mechanism, regulation, links to disease, industrial applications* (Springer, Dordrecht, 2014), pp. 105–134
55. H. Nadaroglu, N.H. Kishali, B. Sever, M.D. Altintop, J Mol Struct **1197**, 386 (2019)
56. R. Demirdag, V. Comakli, M. Kuzu, E. Yerlikaya, M. Şentürk, J Biochem Mol Toxicol **29**, 123 (2015)

57. M. Kuzu, A. Özkaya, Z. Şahin, Ü. Dağ, V. Çomaklı, R. Demirdağ, Turkish J Phamaceutical Sci **14**, 9 (2017)
58. I. Kizilcikli, Y.D. Kurt, B. Akkurt, A.Y. Genel, S. Birteksöz, G. Ötük, B. Ülküseven, Folia Microbiol Praha **52**, 15 (2007)
59. K.S.A. Melha, J Enzyme Inhib Med Chem **23**, 4 (2008)
60. E. Pahontu, F. Julea, T. Rosu, V. Purcarea, Y. Chumakov, J Cell Mol Med **19**, 865 (2015)
61. F. Bisceglie, C. Bacci, A. Vismarra, E. Barilli, M. Pioli, J Inorg Biochem **203**, 110888 (2020)
62. E.B. Noruzi, B. Shaabani, S. Geremia, N. Hickey, P. Nitti, H.S. Kafi, Molecules **25**, 370 (2020)
63. Z. Zu, R. McKendry, C.L. Chavez, *Signaling in copper ion homeostasis* (Elsevier BV, Amsterdam, 2000), pp. 293–300
64. F. Xie, F. Peng, J Fluoresc **28**, 89 (2018)

Affiliations

Asuman Ucar[1] · Mukerrem Findik[2] · Muslum Kuzu[3] · Suray Pehlivanoglu[4] · Ulku Sayin[5] · Zafer Sayin[6] · Emine Guler Akgemci[7]

✉ Asuman Ucar
asucar340@gmail.com

[1] Department of Science Education, Education Faculty, Agri Ibrahim Cecen University, Agri, Turkey

[2] Department of Chemistry Education, Research Laboratory, Ahmet Kelesoglu Education Faculty, Necmettin Erbakan University, Konya, Turkey

[3] Department of Nutrition and Dietetics, Health Sciences Faculty, Karabuk University, Karabuk, Turkey

[4] Department of Molecular Biology and Genetics, Faculty of Science, Necmettin Erbakan University, Konya, Turkey

[5] Physics Department, Science Faculty, Selcuk University, Campus, Konya, Turkey

[6] Department of Microbiology and Immunology, Faculty of Veterinary Medicine, Selcuk University, Konya, Turkey

[7] Department of Chemistry Education, Ahmet Kelesoglu Education Faculty, Necmettin Erbakan University, Konya, Turkey